Neutron beam monitor based on 10B-RPC with delay line

Petrova M.O.*, Bogdzel A.A., Milkov V.M., Bodnarchuk V.I., Daulbaev O., Bulatov K. V., Kurilkin A.A., E.I. Litvinenko

*mbelova@jinr.ru

Abstract

The scattering and absorption of neutron beams by the structural components of the detector are explored using the Monte Carlo method. The X-ray reflectometry curves for manufactured converter films have been obtained and analyzed. Measuring the gamma-ray spectrum of the neutron conversion reaction using boron has been done. The results of measurements using a CAEN6730 digitizer with a 1D 10B-RPC detector and a 252Cf laboratory source are presented.

Introduction

In this paper we report the results of a study of the applicability of 10B-RPC for thermal neutron detection and estimation of the neutron detection efficiency.

X-Ray reflectometry

In order to create a prototype for the 10B-RPC, a series of converter films were deposited on glass float substrates in the ESS Detector Coatings Workshop at Linköping University using a Chewbacca CemeCon CC800/9 DC magnetron at a temperature of 400 °C. The films were applied in three different thicknesses: 0.5, 1, and 2 microns. To determine the structural and density characteristics of the films, we employed a PANalytical Empyrean X-ray diffraction instrument, whose tube material was copper. The wavelength ratio of the K-alpha1 and K-alpha2 lines was set to 0.5 (λ(K-alpha1) = 1.540598 Å, λ(K-alpha2) = 1.544426 Å). The least squares fitting analysis of reflectivity curves (fig.1) revealed that the film exhibits a density of 2.47 g/cm3 and is a superlattice, with characteristic layer thicknesses of 6.4 nanometers and 4.3 nanometers. Peaks corresponding to these thicknesses are observed, in accordance with the Wolfe–Bragg condition.

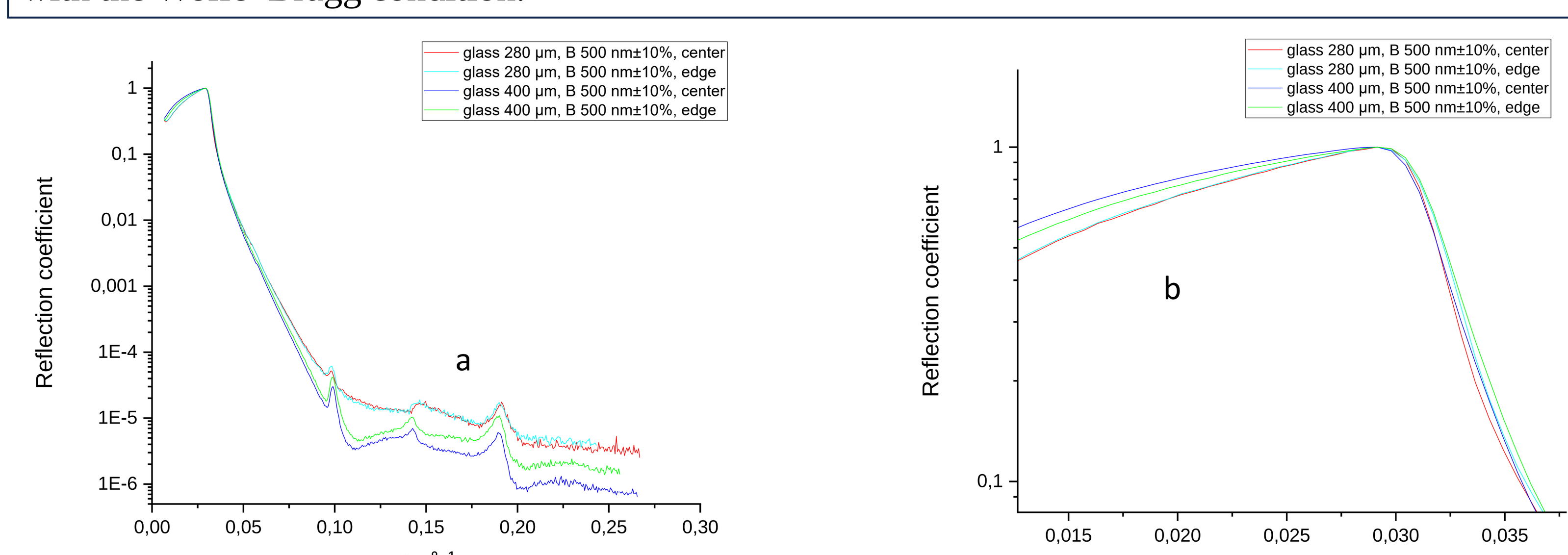

Fig.1 X-ray reflectivity curves of 10B4C films

Geant4 Monte-Carlo simulation

The physical processes implemented in Geant4 were:
i. Standard electromagnetic, hadronic and transportation models.
ii. For neutrons, the low energy processes were implemented using the Evaluated Neutron Data Library G4ENDL, based on the ENDF/B-VI cross-section evaluation.
The General Particle Source (GPS) tool, available in the Geant4 distribution, was used to define the neutron source. It was an user-adaptation with the following features: the simulated structure (fig.2) was irradiated by a monoenergetic broad neutron beam focused on the detector surface, sufficiently far D=100 cm (fig.3) in such a way that the irradiation direction can be considered normally incident on the detector components. Structure In each simulation run, the source emitted 10^6 incident monoenergetic neutrons, towards the detector's entrance face. The statistical relative uncertainties were less than 0.1%. Fig. 4 shows the energy deposition spectrum from the products of the thermal neutron conversion reaction by 10B4 films of various thicknesses with a density of 2.47 g/cm3. The "weak" peak in the low-energy region is due to the photoelectric effect electrons from the interaction of gamma quanta of the conversion reaction with structural materials of detector. A peak with a maximum in the region of 180 keV corresponds to the energy release from alpha and lithium. When integrating the energy deposition spectra obtained for different film thicknesses and neutron wavelengths with different thresholds, dependences of conversion efficiency as a function of wavelength were obtained (Fig.5) and as a function of the thickness of the 10B4C film (Fig.6). In addition, the absorption and scattering of the neutron beam by the structural materials of the detector was evaluated (Fig.6)

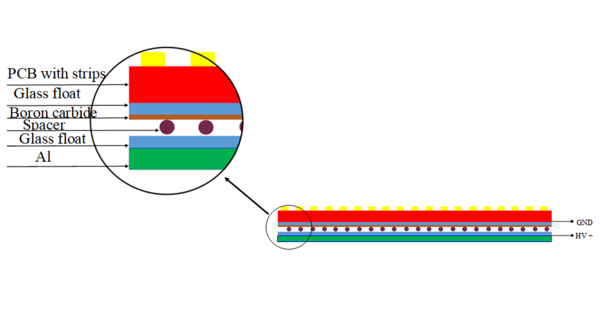

Fig.2. Simulated detector structure

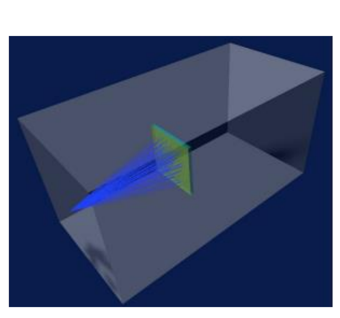

Fig.3 Geant4 model

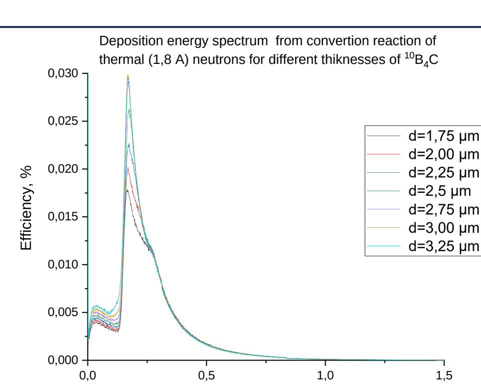

Fig.4 Deposition energy in 249 μm of C2H2F4 at normal conditions

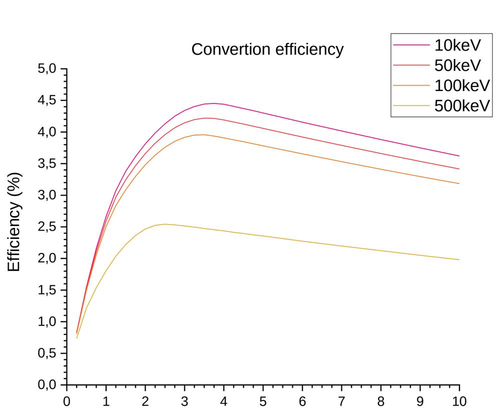

Fig.5 The conversion efficiency of normally incident thermal neutrons (1.8 Å) for 10B-RPC as a function of the thickness 10B4C

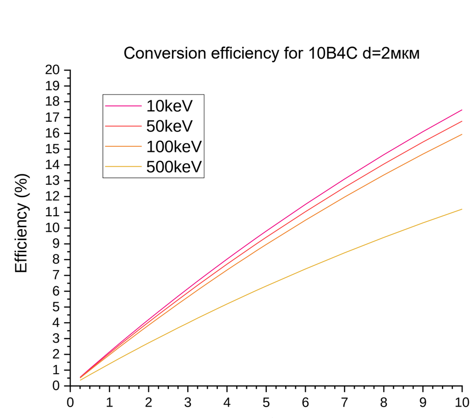

Fig.6 The neutron conversion efficiency for 10B-RPC as a function of the neutron wavelength at a thickness of 10B4C 2 μm

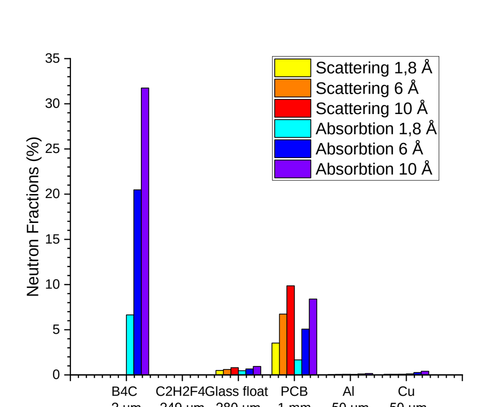

Fig.7 The fractions of scattered and absorbed neutrons by structural materials of 10B-RPC

Spectrum of conversion gamma quanta

The capture of the thermal neutron by 10B leads to the decay of the compound nucleus through two channels:

$^{10}B + n \rightarrow \alpha + {}^{7}Li + \gamma$ (93.7%), (1)

$^{10}B + n \rightarrow \alpha + {}^{7}Li$, (6.3 %)

As can be seen from (1), in addition to heavy charged particles, in ~ 94% of cases the conversion reaction is accompanied by the emission of a gamma quantum with an energy of 478 keV. The maximum Doppler shift of this transition was calculated and amounted to 7.6 keV. Its measurement was carried out with a 252Cf laboratory neutron source surrounded by a plastic spherical moderator. The glass with 10B4C was located directly on the germanium spectrometer Canberra GC10021, the spectrometer and the glass with the converter were surrounded from gamma of 252Cf by a 1 cm thick lead cap. The measurement results are shown in Fig.8

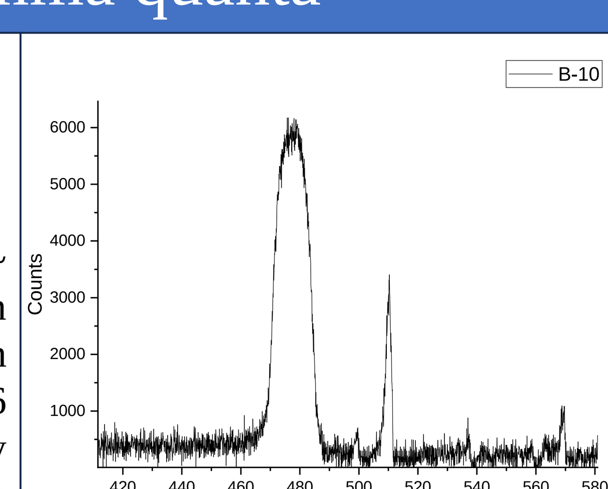

Fig.8 Gamma quanta spectrum of neutron conversion by 10B measured by GC10021

Measuring results of 10B-RPC with 252Cf

The electron path is made equal to the width of the gas gap by grounding the electrode without a converter film to increase the reliability and efficiency of registration. The movement of primary ionization produced avalanche, the Townsend coefficient obtained in the Magboltz package for C2H2F4 under normal conditions is shown in Fig.9. The movement of the avalanche charge induces a signal (Fig.10) to the strips (Fig.11) connected to the delay line. The study of the prototype's operability was also performed using a 252Cf laboratory source surrounded by a plastic spherical moderator, the measurement scheme is shown in Fig.12. In addition to the neutron source, the measurements used: a tetrafluoroethane (C2H2F4) with a rotameter to control gas flow, the purge rate was 3 cm3/min; high voltage source and digitizer from CAEN; 3 preamps - 1 – anode with K = 800, which is a trigger and opens a 200 ns window for signals from delay lines, and 2 – from the ends of the delay line with K = 1200. Coils 95 nGn and capacitors 39 pF from Murata were used for the delay line. The dimensions of the detector's working area were 75 × 150 mm2, and the total delay line duration was 108 ns. The implementation of the delay line method makes it possible to significantly reduce the number of required recording channels while maintaining high spatial resolution, which, when implementing the leading edge method, is determined by the digitizer sampling rate, in CAEN6730 it is 500 MHz. The counting characteristic of the detector is shown in Fig. 13. Due to the relatively sensitivity RPC to cosmic and gamma radiation, distribution maps PSD_q , sum_q, sum_PSD were studied, where PSD =(Q_long-Q_short)/Q_long, and sum is the sum of the signal arrival time at both ends of the delay line, ns, q is the anode charge, fQ. Fig.14 shows that the most optimal is the use of the sum_PSD cut which allows to determine neutron events while preserving more than 87% of all recorded events. The registration efficiency of the 10B-RPC+CAEN6730 system is 2.3% in terms of the entire plane, and the time resolution is1.8 ns. Fig.15 presents the measurement results (24h) of the cadmium mask.

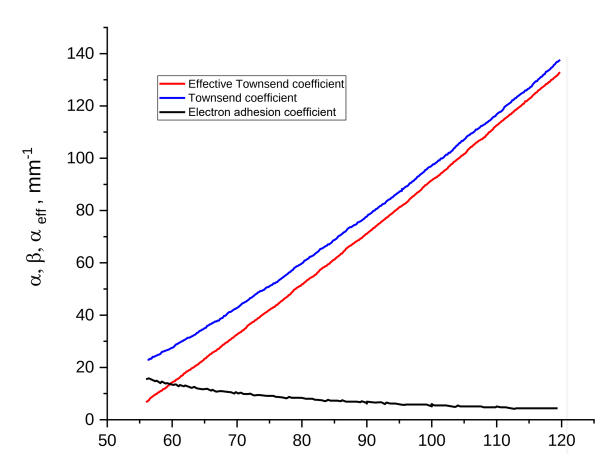

Fig.9 Gas coefficients

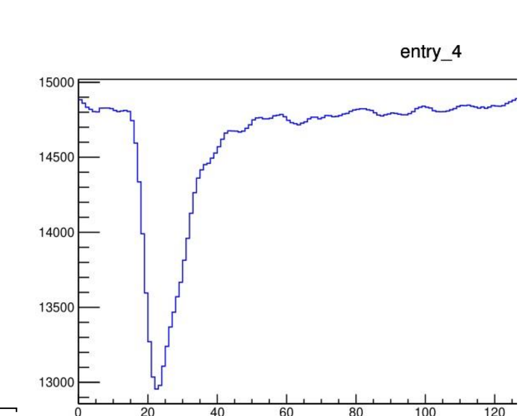

Fig.10 10B-RPC signal

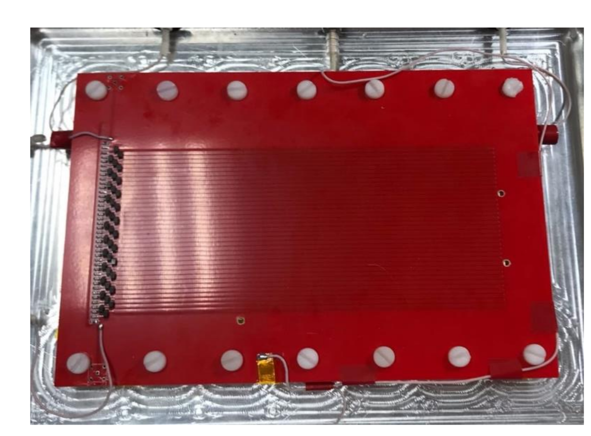

Fig.11 10B-RPC

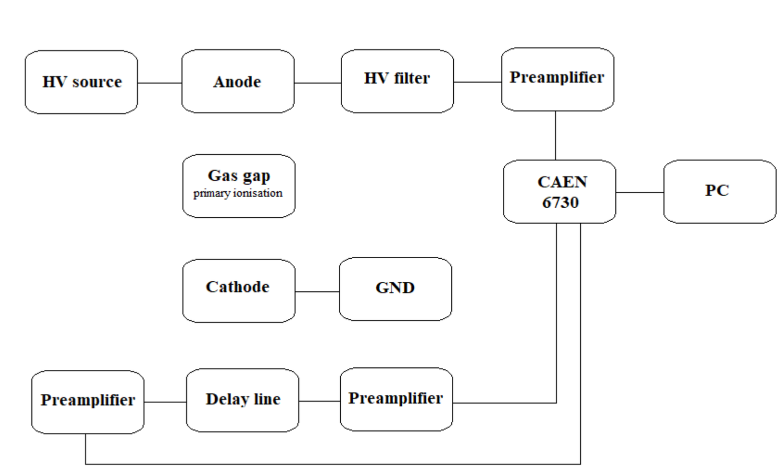

Fig.12 Measuring scheme

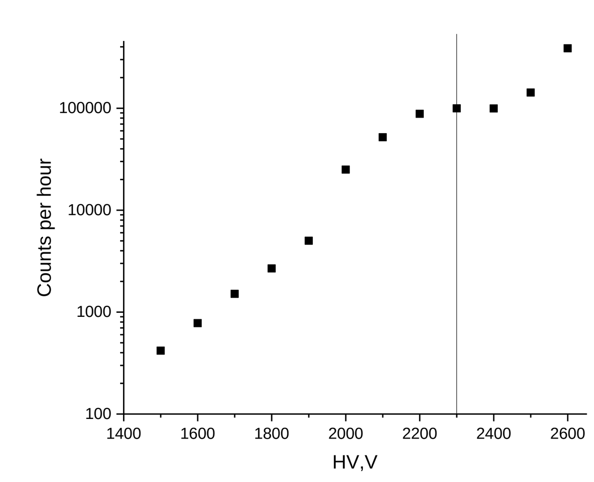

Fig.13 Counting characteristic

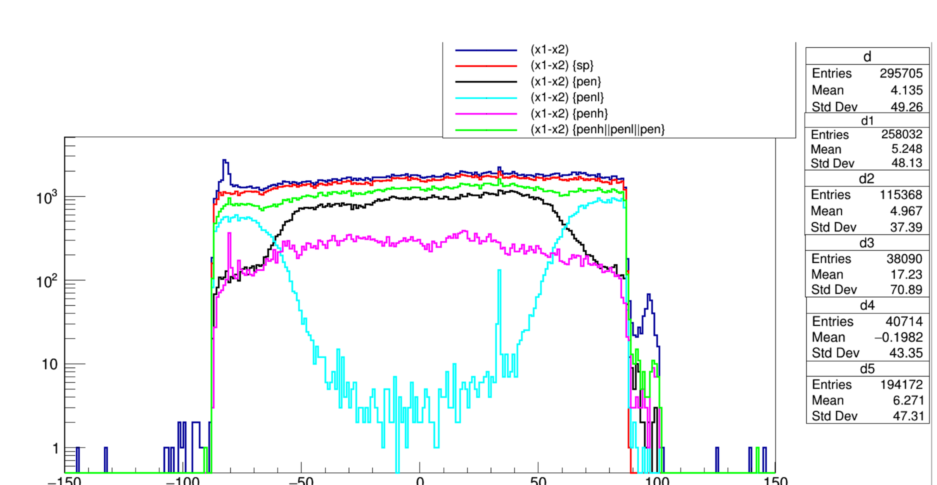

Fig.14 1D quasi-uniform illumination with different cuts

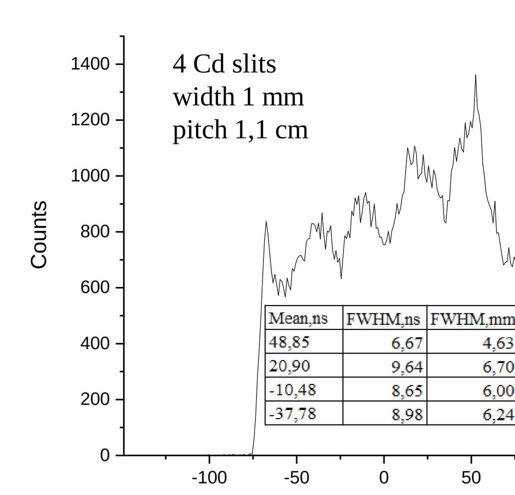

Fig.15 Results of Cd mask 24 h measurement

Conclusions

In this work the applicability of 10B-RPC as a slow neutron detector was demonstrated, the main parameters of the system were determined and a method for selecting neutron events was developed. Low cost, scalability and implementation of inclined geometry make the 10B-RPC a promising detector for covering large areas of cold reflectometers.

References

[1] A. Blanco et al., *Nucl. Instr. and Meth.* A, 602 (2009) 691-695. DOI: https://doi.org/10.1016/j.nima.2008.12.091
[2] R. SANTONICO and R. CARDARELLI, Nuclear Instruments and Methods 187 (1981) 377.
[3] R. Cardarelli et al, Nucl. Instr. and Meth. A 333 (1993) 399-403.
[4] Xiao-Lin ZHOU, Sow-Hsin CHEN, Physics Reports 257 (1995) 223-348
[5] N.V. Borovikova et al. Letters 38(3) (1983) 168.
[6] P. Kok, PhD Thesis defense: Jul, 1986; Report number: ECN-184)
[7] S.F. Mughabghab, M. Divadeenam, and N.E. HoxlenAcademic Prets, New York, 1981, pt. A.
[8] A.J. Deruytter, and P. Pelfer; J. Nucl. Energy 21 (1967) 833.
[9] Петрова М.О., С.В. Антонов, В.И. Боднарчук, Прикладная физика и математика,2023, В.5, стр.57-62, DOI:10.25791/pfi m.06.2023.1282
[10] Caen User Manual UM5960, CoMPASS: Multiparametric DAQ Software for Physics Applications. Rev. 20 - September 23rd, 2022